Proceedings of the Sixth International Conference on
Railway Technology: Research, Development and Maintenance
Edited by: J. Pombo
Civil-Comp Conferences, Volume 7, Paper 3.17
Civil-Comp Press, Edinburgh, United Kingdom, 2024
ISSN: 2753-3239, doi: 10.4203/ccc.7.3.17

Dynamic Modelling of the Aerodynamic Characteristics of a 600km/h High-Speed Magnetic Levitation Train Traversing a Tunnel

S. Xu and L. Zhang

**School of Traffic & Transportation Engineering,
Central South University, China**

Abstract

This paper adopts the unique dynamic model test system for aerodynamic characteristics of high-speed magnetic levitation trains with speeds of 600 km/h and above of Central South University to carry out dynamic model test and research on eight different head types of high-speed magnetic levitation trains in open line operation, rendezvous, single-car passing through tunnels and rendezvous in tunnels, etc., and to obtain and analyse the resistance of different head types of trains in open line operation, the wind of the train, the characteristics of the rendezvous pressure wave, the pressure wave propagation law of the surface of the train and the surface of the tunnel when the train passes through the tunnel, as well as to analyse the micro-air pressure wave propagation characteristics of the train caused by a single-car passing through the tunnel. When the train surface and the tunnel surface pressure wave propagation law, and analysed the train single car through the tunnel caused by the micro-barometric pressure wave propagation characteristics, for high-speed magnetic levitation train design and operation to provide a scientific basis.

Keywords: high-speed magnetic levitation train, 600 km/h dynamic model test bed, rendezvous pressure wave, tunnel aerodynamic effects, micro-pressure wave, pressure distribution.

1 Introduction

High-speed magnetic levitation trains generate large transient pressures when passing through tunnels, which can cause instability to the internal structure of the levitation

train and the tunnel, as well as affecting the comfort of the passengers, such as tinnitus and other medical problems [1,2]. Ozawa [3] first raised the environmental issue of micro barometric pressure waves in 1979.

With the continuous progress of technology, the safety, comfort and speed of rail transport have been significantly improved. In this process, maglev trains have emerged as a new type of high-speed transport. Compared with traditional wheeled trains, maglev trains have many advantages such as lower total resistance, smaller noise output and more spacious acceleration space [4]. The Shanghai Maglev line in China has now achieved impressive commercial operating speeds of up to 430 kilometres per hour. In comparison, civilian aircraft typically travel at speeds of 800 km/h, so there is a significant speed gap between high-speed trains and aircraft. However, the demand for travel speeds does not always match transport capacity exactly. As a result, the goal of establishing transport systems on land that enable operation at speeds of 600 km/h will still be pursued globally, which is a crucial goal [5].

However, at higher speeds, aerodynamic effects may pose serious challenges to the stability and safety of maglev trains [6,7]. Firstly, micro-pressure waves and alternating pressures generated by the coupling between the train and the tunnel can reduce the fatigue life of the structural materials, as well as significantly affect passenger comfort. Secondly, lateral pressure waves generated when trains pass each other may lead to serpentine motion, which in turn may lead to train rollover. Finally, due to the viscous nature of air, slipstreams induced by high-speed train motion may seriously threaten the safety of roadside personnel [8]. Therefore, this paper can provide some aerodynamic parameters for the study of high-speed maglev trains passing through tunnels.

2 Methods

2.1 Similarity of model tests

Train aerodynamic performance simulation model test with air as the test medium, and the actual train running environment medium, simulation test and the actual train running air flow state similarity is directly related to the correctness of the simulation test results. Therefore, the similarity between the model scale and running speed selected for the simulation test and the actual air flow state is a problem we must be concerned about.

From the similarity theorem, in the model test, first of all must ensure that the model and the physical two flow fields are similar, the test should be measured in the similarity criterion or the physical quantities contained in the similarity criterion, the test data in accordance with the similarity criterion for the organisation of the test data, so that the model test data can be used in the physical flow field[9].

2.2 Dynamic modelling test methods

This paper adopts the dynamic model experimental method. The dynamic model test system consists of test bench, power system, acceleration system, control system, test system, braking system, data processing system and test model.

Dynamic model ejection test basic principle (Figure 1)[1]: in the simulation of the end of the line pulling the traction trolley and its connected to the dynamic model train backward movement, the control system to control the size of the traction trolley by the tension (through the tension can be approximated to estimate the running speed of the model train), at the same time, driven by the lower level of the test bed of the power transmission trolley is also backward movement, so that the rope is gradually tightened when the tension reaches the specified value, the control system to stop backward Pull, the model train in the state to be launched, traction trolley unhooking device control solenoid valve action, release the unhooking device, the ejection device rebound drive traction power transfer trolley and moving model train movement, moving model train traveling to the entrance of the test section, and power transfer trolley automatically separated, moving model train was ejected, relying on the inertia of the track along the unpowered high-speed running.

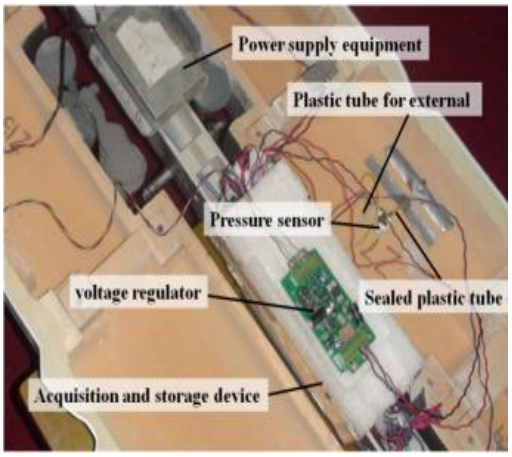

Figure 1: System for measuring pressure on the train model's surface.

2.3 Models

All the train models used are shown in Figure 2. The adopted tunnel model is shown in Figure 3. The surface pressure sensors of the adopted tunnels are shown in Figure 4.

Figure 2: Eight head models of high-speed magnetic levitation trains.

Figure 3: Model of a tunnel with a cross sectional area of 100 square metres.

Figure 4: Tunnel model surface pressure sensor deployment.

2.3 Measurement point arrangement

Twelve pressure monitoring points were laid on the surface of the high-speed magnetic levitation train, and the arrangement of the surface measurement points is shown in Figure 5; seven pressure monitoring points were laid on the tunnel wall, and the setup of the tunnel wall measurement points is shown in Figure 6.

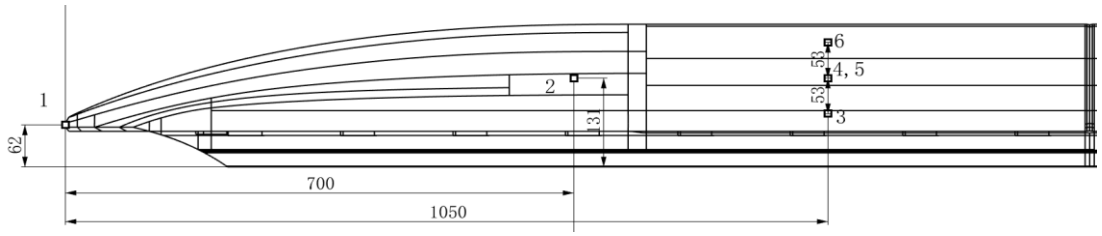

(a) EMU1 Head

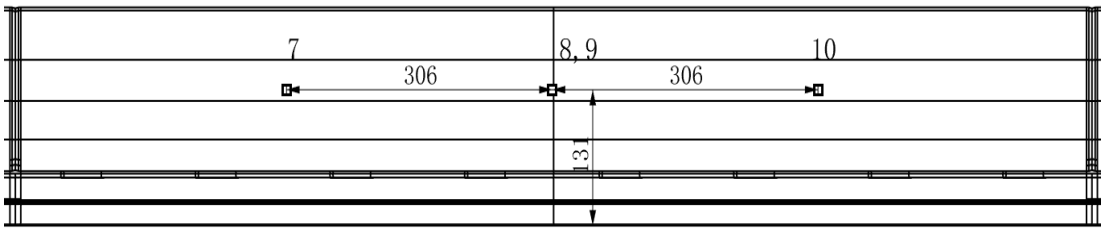

(b) EMU1 Middle

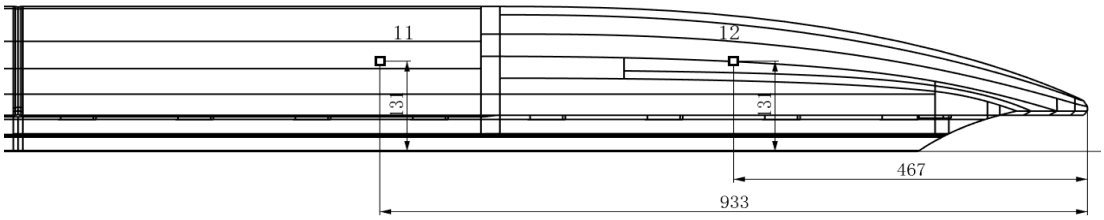

(c) EMU1 Tail

Figure 5: Arrangement of measurement points on the body surface.

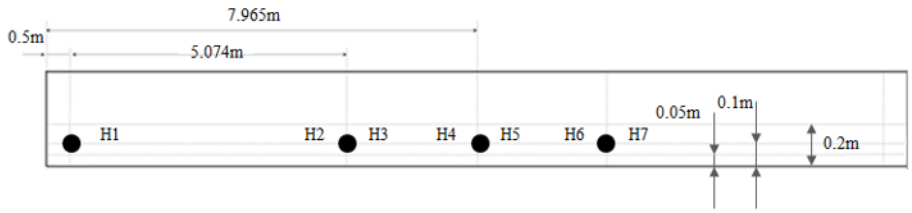

Figure 6: Layout of tunnel measurement points.

3 Results

3.1 Speed effects

To analyse the pressure changes on the train surface, tunnel wall measurement points when passing through an 80m2 tunnel at speeds of 350km/h, 430km/h, 550km/h and 600km/h for the TR08, EMU1 and EMU2 models, respectively.

Figure 7 shows the EMU1 high-speed magnetic levitation train at 600km/h through the tunnel, respectively, the body surface of the No. 2 measurement point pressure change time curve, the zero position of the time in the figure for the train nose burst into the tunnel now.

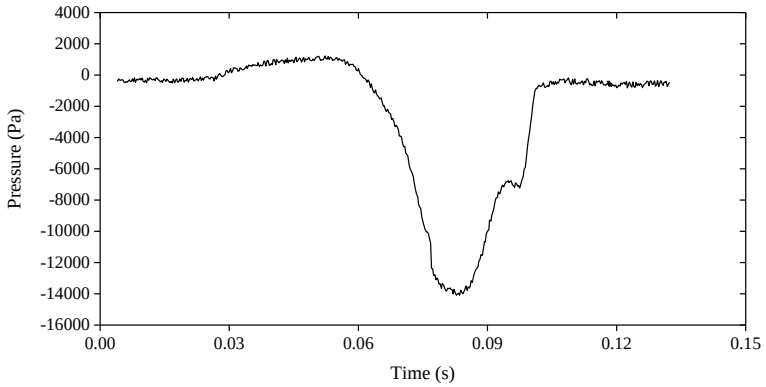

Figure 7: Time course curve of pressure change at measuring point No. 2 on the train surface.

In order to facilitate the comparison of the aerodynamic characteristics of high-speed magnetic levitation train single-vehicle over the tunnel, three models of the car body surface measurement point pressure extreme value for comparison and analysis, due to the car body surface measurement point in the nose tip position is located in the flow field stationary point or stationary point of the surrounding, the maximum positive pressure value and the pressure peak peak value is much larger than the other positions of the car body, the measurement point cannot be characterised by the overall situation of the whole car surface measurement point pressure extreme value, so the train were extracted without the nose tip measurement point Therefore, the pressure extremes of the surface measurement points without the nose tip measurement point are extracted separately, as shown in Tables 1 . Figures 8 show the change rule of the pressure extreme value of the surface measuring point of EMU1 high-speed magnetic levitation train with the vehicle speed in the two cases.

Models	Speed 350km/h			Speed 430km/h		
	MAXPmax	*MINPmin*	*MAX⊿P*	*MAXPmax*	*MINPmin*	*MAX⊿P*
TR08	345	-4209	4503	543	-6735	7254
EMU1	346	-4267	4511	520	-6800	7165
EMU2	372	-4260	4550	554	-6783	7170
Models	Speed 550km/h			Speed 600km/h		
	MAXPmax	*MINPmin*	*MAX⊿P*	*MAXPmax*	*MINPmin*	*MAX⊿P*
TR08	874	-12002	12381	1267	-15178	15342
EMU1	897	-12177	12475	1120	-15143	15344
EMU2	981	-12161	12524	1228	-15140	15343

Table 1: Comparison of pressure extremes at body surface measurement points without nose tip T-1 (Pa).

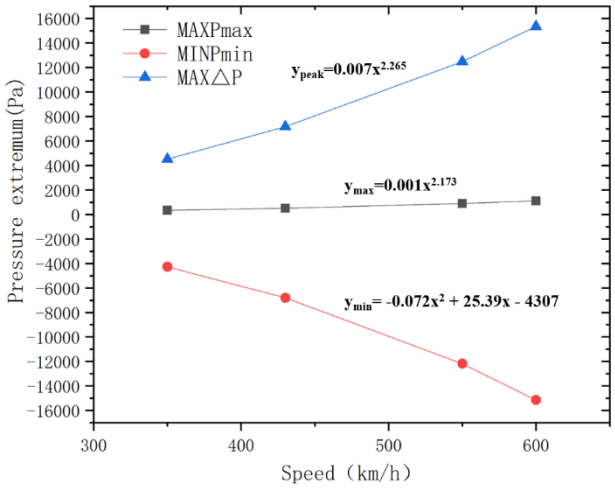

Figure 8: Change pattern of pressure extremes with vehicle speed at body surface measurement points (excluding the nose tip T-1 measurement point).

As can be seen from the comparisons of the above graphs, the difference between the extreme values of the surface pressures caused by the three types of vehicles entering the tunnel is relatively small, with a difference of less than 3%. The maximum value of the positive peak pressure at each measurement point increases with the speed of the vehicle in an approximate second-square relationship, the maximum value of the peak-to-peak value increases in an approximate second-square relationship, and the minimum value of the pressure at each measurement point decreases with the speed of the vehicle in an approximate quadratic polynomial relationship.

Figure 9 shows the EMU1 high-speed maglev train passing through the tunnel at a speed of 600km/h, the pressure change time curve of the tunnel wall No. 2 measuring point, the zero position of the time in the figure is the moment when the nose of the train protrudes into the tunnel.

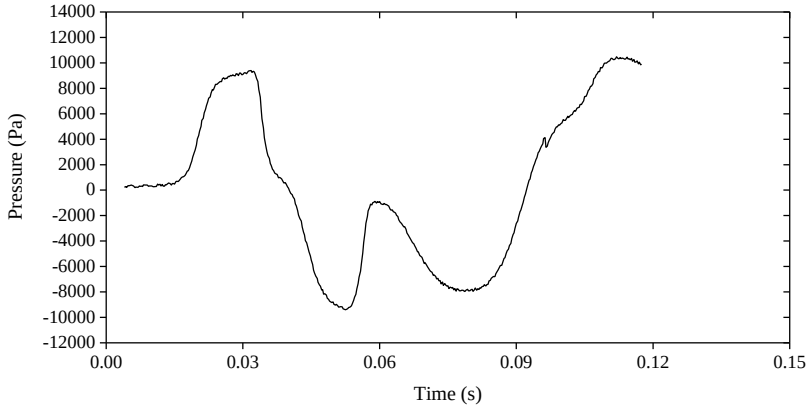

Figure 9: Time course of pressure change at measurement point 2 on the tunnel wall.

In order to facilitate the comparison of the pressure change of the tunnel wall surface measurement points, the pressure extreme value of each measurement point of the tunnel wall surface under different working conditions is extracted, as shown in Table 2. Figure 10 shows the change rule of the pressure extreme value of the measuring point of the tunnel wall with the speed of EMU1 high-speed magnetic levitation train when it passes through the tunnel.

Models	Speed 350km/h			Speed 430km/h		
	MAXPmax	*MINPmin*	*MAX△P*	*MAXPmax*	*MINPmin*	*MAX△P*
TR08	4596	-4633	9229	7047	-7161	14165
EMU1	4442	-4412	8808	6999	-7051	14050
EMU2	4509	-4498	8909	6944	-7076	14007
Models	Speed 550km/h			Speed 600km/h		
	MAXPmax	*MINPmin*	*MAX△P*	*MAXPmax*	*MINPmin*	*MAX△P*
TR08	12112	-12867	24977	15203	-15932	31135
EMU1	12044	-12525	24569	15005	-15479	30484
EMU2	12084	-12615	24559	15193	-15582	30545

Table 2 Comparison of extreme values of tunnel wall pressure (Pa).

.

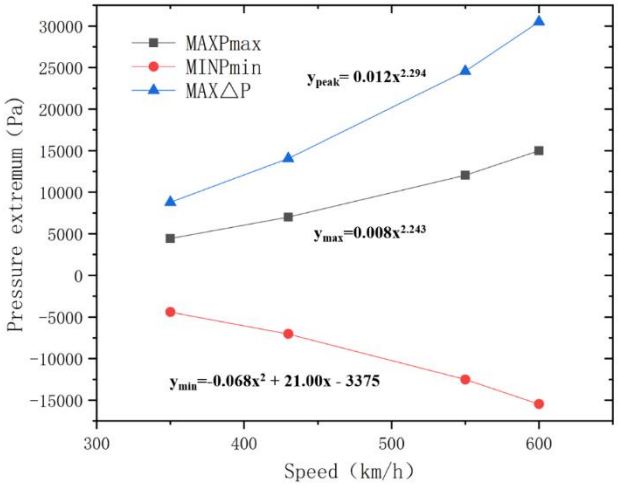

Figure 10: The change rule of pressure extreme value of tunnel wall measuring point with the speed of vehicle.

It can be seen from the comparison of the extreme value of the pressure at the tunnel wall measurement point that when the high-speed maglev train passes through the 80m2 tunnel at a speed of 430km/h and above, the absolute extreme value of the maximum and minimum values of the pressure at the tunnel wall measurement point is greater than 6000Pa, and the maximum of the positive peak value and the maximum of the peak pressure peak value increase with the train speed in an approximate 2.2-polynomial relationship, whereas the extreme value of the minimum value decreases with the train speed in a quadratic polynomial relationship decreases.

3.2 Impact of the model

Analyse the pressure changes on the train surface, tunnel wall measurement points and tunnel exit micro-barometric pressure waves when the eight models of TR08, EMU1 to EMU7 pass through the 80m2 tunnel at speeds of 430km/h and 550km/h, respectively. The numerical values of train surface pressure for the eight models passing through the 80m2 tunnel at speeds of 430km/h and 550km/h are shown in Table 3, and Figure 11 shows the histogram for the 550km/h speed.

Models	Speed 430km/h			Speed 550km/h		
	MAXPmax	*MINPmin*	*MAX△P*	*MAXPmax*	*MINPmin*	*MAX△P*
TR08	543	-6735	7254	874	-12002	12381
EMU1	520	-6800	7165	897	-12177	12475
EMU2	554	-6783	7170	981	-12161	12524
EMU3	522	-6824	7175	785	-12138	12237
EMU4	515	-6791	7167	757	-11913	12670
EMU5	529	-6825	7194	762	-11761	12072
EMU6	528	-6827	7187	754	-11738	12088
EMU7	634	-6884	7371	760	-11827	12236

Table 3: Comparison of pressure extremes at body surface measurement points without nose tip T-1 (Pa).

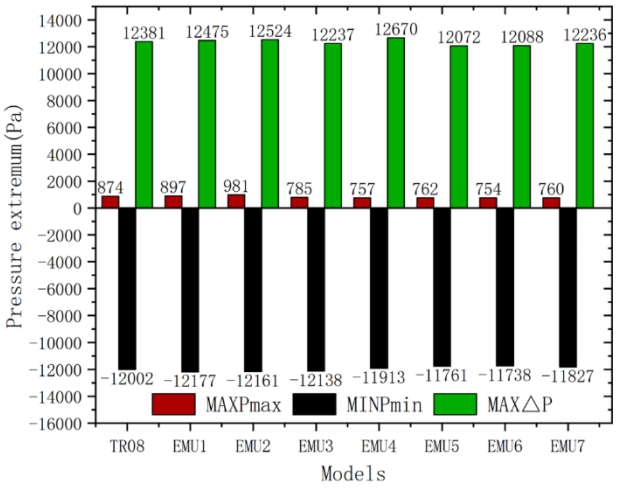

Figure 11: Comparison of pressure extremes at body surface measurement points for eight models, vehicle speed 550km/h, without nose tip T-1 measurement point (Pa).

Therefore, at 430km/h, the difference between the maximum positive peak pressure of different models is only 119Pa, and the difference between the minimum negative peak pressure and the maximum peak pressure is 2.1 per cent and 2.7 per cent respectively; at 550km/h, the difference between the maximum positive peak

pressure of different models is only 224Pa, and the difference between the minimum negative peak pressure and the maximum peak pressure is 3.6 per cent and 4.7 per cent respectively.

In order to facilitate the comparison of the aerodynamic characteristics of high-speed magnetic levitation train single-vehicle tunnel, eight models through the tunnel when the tunnel wall measurement point pressure extreme values for comparison and analysis, shown in Table 4. Figure 12 shows 550km/h under the tunnel wall surface measurement point maximum pressure positive peak value, minimum pressure negative peak value and maximum pressure peak peak value of the comparison bar graph.

车型	车速 430km/h			车速 550km/h		
	MAXPmax	*MINPmin*	*MAX⊿P*	*MAXPmax*	*MINPmin*	*MAX⊿P*
TR08	7047	-7161	14165	12112	-12867	24977
EMU1	6999	-7051	14050	12044	-12525	24569
EMU2	6944	-7076	14007	12084	-12615	24559
EMU3	7016	-6941	13957	12092	-12554	24647
EMU4	6898	-6824	13722	12018	-12470	24488
EMU5	6981	-7048	14029	12021	-12513	24534
EMU6	6993	-7060	14053	12050	-12541	24591
EMU7	7166	-7164	14329	12101	-12624	24725

Table 4 Comparison of pressure extremes at tunnel wall measurement points (Pa).

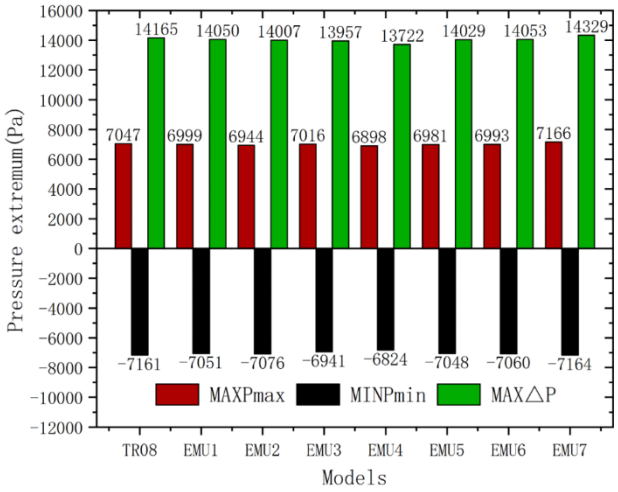

Figure 12: Extreme values of pressure (Pa) at tunnel wall measurement points when a train passes through a tunnel at a speed of 550km/h.

From the above graphical data, it can be seen that at a speed of 430km/h, when different models pass through the tunnel, the difference between the maximum positive peak pressure, the minimum negative peak pressure and the maximum peak

pressure at the tunnel wall measurement point is 3.7%, 4.7% and 4.2%, respectively; at a speed of 550km/h, the difference between the maximum positive peak pressure, the minimum negative peak pressure and the maximum peak pressure at the tunnel wall measurement point is 0.8%, 3.1% and 2.0% respectively.

3.3 Influence of Tunnel Sections

To analyse the pressure variations at the train surface and tunnel wall measurement points for the TR08, EMU1 and EMU2 models when passing through tunnels of 80 m2, 100 m2 and 140 m2 at a speed of 550 km/h. The body surface pressures are shown in Table 5 and Figure 13

Models	80 square meters			100 square meters		
	MAXPmax	*MINPmin*	*MAX △P*	*MAXPmax*	*MINPmin*	*MAX △P*
TR08	874	-12002	12381	646	-9348	9604
EMU1	897	-12177	12475	659	-9450	9684
EMU2	981	-12161	12524	664	-9435	9686
Models	140 square meters					
	MAXPmax		MINPmin		MAX△P	
TR08	372		-6544		6592	
EMU1	360		-6445		6619	
EMU2	369		-6505		6679	

Table 5: Comparison of pressure extremes at body surface measurement points without nose tip T-1 (Pa).

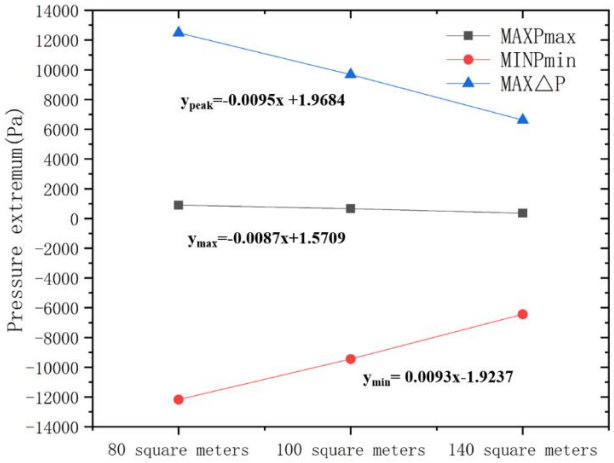

Figure 13: Change pattern of pressure extremes with vehicle speed at body surface measurement points (excluding the nose tip T-1 measurement point).

The maximum value of the positive peak pressure at each measurement point decreases approximately linearly with area, the maximum value of the peak-to-peak value decreases approximately linearly, and the minimum value of the pressure at the measurement point increases approximately linearly with area.

Tunnel wall pressures are shown in Table 6 and Figure 14.

Models	80 square meters			100 square meters		
	MAXPmax	*MINPmin*	*MAX △P*	*MAXPmax*	*MINPmin*	*MAX △P*
TR08	12112	-12867	24977	9468	-10015	19461
EMU1	12044	-12525	24569	9396	-9736	19133
EMU2	12084	-12615	24559	9397	-9815	19116
Models	140 square meters					
	MAXPmax		MINPmin		MAX△P	
TR08	6517		-6946		13454	
EMU1	6466		-6785		13251	
EMU2	6494		-6806		13234	

Table 6 Comparison of extreme values of tunnel wall pressure (Pa).

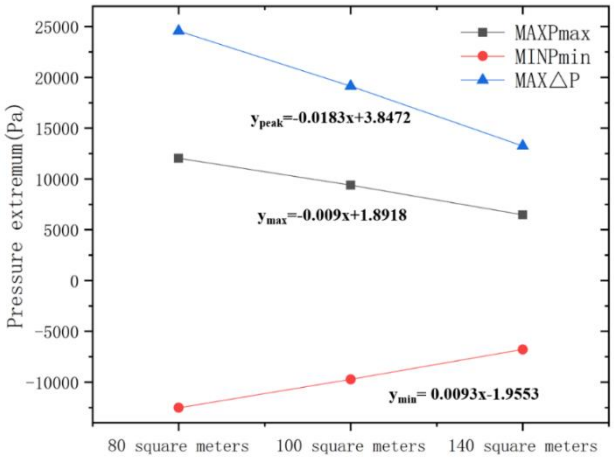

Figure 14: The change rule of pressure extreme value of tunnel wall measuring point with the speed of vehicle.

The absolute extreme values of the maximum and minimum values of the pressure at the measurement points on the tunnel wall are greater than 12,000 Pa. The maximum value of the positive peak and the maximum value of the peak pressure decrease with the approximate linear relationship of the train speed, while the extreme

value of the minimum value increases with the speed of the train in a linear relationship.

4 Conclusions and Contributions

1: when the vehicle speed increases, the maximum value of the positive peak pressure of the vehicle body surface pressure and tunnel wall pressure increases with the speed of the approximate relationship of the second power, the maximum value of the peak value of the approximate relationship of the second power, while the minimum value of the pressure at the measurement point decreases with the speed of the approximate relationship of the quadratic polynomial.

2: the difference between the minimum negative peak value and the maximum peak value of the pressure on the surface of the car body of different models is 2.1% and 2.7% respectively, and the difference between the minimum negative peak value and the maximum peak value of the pressure on the tunnel wall of different models is 3.6% and 4.7% respectively.

3: when the tunnel area increases, the maximum value of the positive peak value of the surface pressure of the car body and the pressure of the tunnel wall pressure and the maximum value of the pressure peak and peak values decrease with the train speed in an approximately linear relationship, while the minimum value of the extreme value decreases with the speed in a linear relationship.

References

[1] L Zhang, M.Z Yang, X.F Liang, J Zhang, “Oblique tunnel portal effects on train and tunnel aerodynamics based on moving model tests”, Journal of Wind Engineering and Industrial Aerodynamics, Volume 167, 128-139, 2017.

[2] R Gawthorpe, "Pressure effects in railway tunnels”, Rail international, 31(4) ,2000.

[3] S Ozawa, "Studies of micro-pressure wave radiated from a tunnel exit", Tetsudo Gijutu Kenkyu Hokoku (Railway Technical Research Repot) ,1979.

[4] S Zhong, B Qian, M Yang, “Investigation on flow field structure and aerodynamic load in vacuum tube transportation system”, Journal of Wind Engineering and Industrial Aerodynamics, 2021.

[5] X Tan, T Wang, B Qian, et al. “Aerodynamic noise simulation and quadrupole noise problem of 600km/h high-speed train”, Ieee Access, 7: 124866-124875,2019.

[6] C J Baker, A Quinn, M Sima, “Full-scale measurement and analysis of train slipstreams and wakes. Part 1: Ensemble averages”, Proceedings of the Institution of Mechanical Engineers, Part F: Journal of Rail and Rapid Transit, 228(5): 451-467,2014.

[7] R S Raghunathan R S, H D Kim, T Setoguchi. “Aerodynamics of high-speed railway train”, Progress in Aerospace sciences, 38(6-7): 469-514.2002.

[8] M Z Yang, S Zhong, L Zhang,"600 km/h moving model rig for high-speed train aerodynamics", Journal of Wind Engineering and Industrial Aerodynamics: The Journal of the International Association for Wind Engineering, 2022.
[9] H.Q Tian. "Train aerodynamics", China Railway Press,2007.